Accepted Manuscript

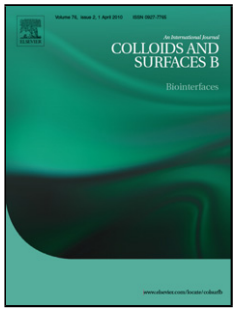

Title: HEXAGONAL PHASE WITH ORDERED ACYL CHAINS FORMED BY A SHORT CHAIN ASYMMETRIC CERAMIDE

Author: F.G. Dupuy S.P. Fernández Bordín B. Maggio R.G. Oliveira

PII: S0927-7765(16)30712-3
DOI: http://dx.doi.org/doi:10.1016/j.colsurfb.2016.10.009
Reference: COLSUB 8190

To appear in: *Colloids and Surfaces B: Biointerfaces*

Received date: 3-5-2016
Revised date: 11-9-2016
Accepted date: 5-10-2016

Please cite this article as: F.G.Dupuy, S.P.Fernández Bordín, B.Maggio, R.G.Oliveira, HEXAGONAL PHASE WITH ORDERED ACYL CHAINS FORMED BY A SHORT CHAIN ASYMMETRIC CERAMIDE, Colloids and Surfaces B: Biointerfaces http://dx.doi.org/10.1016/j.colsurfb.2016.10.009

This is a PDF file of an unedited manuscript that has been accepted for publication. As a service to our customers we are providing this early version of the manuscript. The manuscript will undergo copyediting, typesetting, and review of the resulting proof before it is published in its final form. Please note that during the production process errors may be discovered which could affect the content, and all legal disclaimers that apply to the journal pertain.

HEXAGONAL PHASE WITH ORDERED ACYL CHAINS FORMED BY A SHORT CHAIN ASYMMETRIC CERAMIDE

F.G. Dupuy[a], S.P. Fernández Bordín[b], B. Maggio[c], and R.G. Oliveira[c]†

a. Instituto Superior de Investigaciones Biológicas (INSIBIO), CONICET-UNT, and Instituto de Química Biológica "Dr. Bernabé Bloj", Facultad de Bioquímica, Química y Farmacia, UNT. Chacabuco 461, T4000ILI – San Miguel de Tucumán, Argentina.

b. Consejo Nacional de Investigaciones Científicas y Técnicas (CONICET), FaMAF, Universidad Nacional de Córdoba, Argentina

c. Centro de Investigaciones en Química Biológica de Córdoba, CIQUIBIC, CONICET and Departamento de Química Biológica, Facultad de Ciencias Químicas, Universidad Nacional de Córdoba, Ciudad Universitaria, X5000HUA, Córdoba, Argentina.

† To whom correspondence should be addressed. oliveira@fcq.unc.edu.ar

Tel: +54-351-5353855

Graphcial abstract

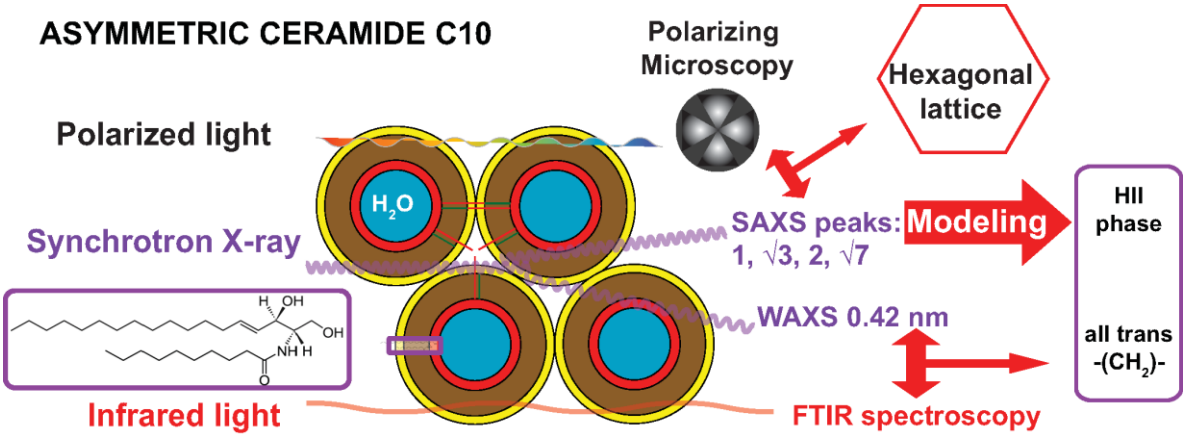

Highlights

We examined the structured of an asymmetric ceramide

A sequence of SAXS diffraction peaks in ratios for hexagonal phase was found

The acyl chains according to WAXS and FTIR are in predominant all trans conformation

The topology corresponds to an inverted (water in oil) micelle

We speculate that the asymmetry of the acyl chains stabilize the structure

Abstract

Ceramides constitute a group of lipids with usually high melting temperature that also favor negative curvature in membranes when mixed with other lipids. The short chain C10:0 ceramide is an asymmetric lipid which consists of an 18 carbon sphingosine base N-acylated with decanoic acid. According to high sensitivity differential scanning calorimetry, it shows a minor exothermic peak at 61 °C and a main endothermic transition at 75 °C. By small angle X-ray scattering and polarized light microscopy we found that, at temperatures below the main transition, the fully

hydrated lipid dispersions are arranged in a tridimensional structure corresponding to an inverted hexagonal phase. Infrared spectroscopy and wide angle X-ray diffraction indicated that the acyl chains of ceramides exhibit a relatively high order in the hexagonal phase. As far as we know, this is the first report of a lipid hexagonal phase having highly ordered acyl chains. Molecular asymmetry due to the different length of the sphingosine and the N-acyl chains of C10:0 ceramide may explain why this novel phase is formed.

Keywords: short chain ceramide, asymmetry, hexagonal phase

1. Introduction

Sphingolipids comprise a vast family of members composed by a long chain aminediol base *N*-linked to a fatty acid through an amide bond. The base most usually found is the 18 carbon sphingosine, with a *trans* double bond at position 4-5, (see Figure 1), which is itself a bioactive lipid; however other variants with shorter or longer hydrocarbon chains, different hydroxylation level and saturation can be found [1-6]. In addition, the *N*-acyl chain can also vary in length (ten in the present case, see Figure 1), hydroxylation and unsaturation level, although long saturated fatty acyl residues are more often encountered in sphingolipids than in glycerol-based lipids; such variations transduce into largely different molecular packing and phase state [7].

In addition, a great variety of polar groups attached to hydroxyl group at position C1 give rise to the different families of sphingolipids: ceramides, with a single hydroxyl group; sphingomyelins, with phosphorylcholine; cerebrosides, with different sugars; gangliosides, with sugars and sialic acid residues [8]; among others.

The chemical variety of the sphingolipids is responsible for the large structural polymorphism observed due to the intrinsic natural curvature that the polar head group, in relation to the hydrocarbon moiety, imposes to the different lipid families [9]. In this regard, while gangliosides with a complex and charged head group self-assemble as micellar structures of different shapes and size [10, 11], sphingomyelins and cerebrosides form stable bilayers [3]. In the case of ceramides, it has been reported that natural extracts of bovine brain and N-palmitoyl-ceramide can form lamellar stackings [12], a feature also induced by other complex glycosphingolipids and some of their mixtures with phosphatidylcholine [13]. However, when mixed with inverted phase-forming lipids such as phosphatidylethanolamine, it was shown that ceramides *N*-acylated with fatty acids equal or longer than 8 carbons decreased the temperature of lamellar Lα to hexagonal II transition [14], suggesting that this ceramide stabilized the negative curvature of membranes. On the other hand, when mixed with dipalmitoyl phosphatidylcholine, an increase of the main transition temperature and reduction of bilayer thickness due to chain interdigitation is induced by egg-Ceramide [15].

Ceramides also display the highest melting transition temperatures described in lipid systems [16-18], owing to tight molecular packing, high Van der Waals interactions and subsequent hydrogen bonding [19]. In bilayer and monolayer membrane model systems, ceramides form highly ordered, solid phases [19-21] and, when mixed with either glycerophospholipids or sphingolipids, induce phase segregation of condensed domains and complex thermograms [18, 22-24]. However it should be pointed out that even the condensed C16:0 ceramide can undergo liquid-expanded to condensed transitions depending on temperature, besides other structural transitions in the condensed state [21]. Also, when the N-acyl chain length of ceramides is shortened to less than 14

carbons, expanded phase and expanded to condensed monolayer phase transition at room temperature have also been found in Langmuir monolayers [21].

In the present work, we studied the phase behavior of an asymmetric ceramide N-acylated with the 10 carbons long decanoic acid, C10:0 ceramide, when dispersed in excess water in bulk. Previous studies [21] have shown C10:0 ceramide is able to form stable monolayers with an expanded to condensed transition at 25 mN.m-1 at 24 °C. Combining differential scanning calorimetry (DSC), small angle X-ray scattering (SAXS), polarized light microscopy (PLM), wide angle X-ray scattering (WAXS) and Fourier transform infrared spectroscopy (FTIR) we could ascertain the presence of a novel lipid phase below the main transition that consists of an inverted hexagonal phase HII in which the acyl chains of C10:0 ceramide are highly ordered. As far as we know, this is the first report of a curved-tubular (hexagonal) phase with ordered acyl chains in pure lipid systems.

2. Materials and Methods

The lipid *N*-decanoyl- *D-erythro*-sphingosine (C10:0 Ceramide, Figure 1) was from Avanti Polar Lipids (Alabaster, Al, USA) and used without further purification. D_2O 99.9 % was from Sigma-Aldrich.

C10:0 Ceramide was difficult to hydrate and generally three to four cycles of freeze and thawing should be carried out from -20 °C to 90°C, followed by extensive bath-sonication. Samples at concentrations higher than 2 $mg.mL^{-1}$ looked opalescent. Unless otherwise indicated, measurements were done in triplicate, with freshly dispersed samples.

DSC was carried out in a MicroCal VP-DSC (MicroCal Llc) at a scanning rate of 0.5 $°C.min^{-1}$ and overpressure of 26 psi. Lipid samples were resuspended in 145 mM NaCl at 0.5 $mg.mL^{-1}$ final concentration and degassed under vacuum. Some loss of material in the walls of the tubes and

sampling syringe was unavoidable, which hampered quantitative treatment of data (enthalpy change determination).

Samples for SAXS measurements were prepared at 5 $mg.mL^{-1}$ in 145 mM NaCl and mounted between mica windows in a liquid cell. Temperature control was achieved by means of an external circulatory bath and a thermocouple, which sensed the block cell. SAXS measurements were carried out at the SAXS-2 beamline at the Brazilian Synchrotron Light Laboratory (LNLS) at Campinas, Brazil. Data was collected by means of a MarCCD detector and radially integrated by using FIT2D V 12.077 from Andy Hammersley at the European Synchrotron Radiation Facility.

The SAXS data were modelled by using the algorithm introduced by Schmidt-Rohr which allows to calculate the scattering intensity profile as a function of scattering vector [25]. Starting from a 2D electron density map made by modelling with SAXS data restrictions, the form factor function *F* was obtained by applying inverse Fourier transform.

Polarizing light microscopy was carried out in an Olympus BX51 system. Small amounts of C10:0 ceramide on a glass slide were covered with coverslips and heated above their main transition. Then, a drop of pre-heated 145 mM NaCl was placed at the edge of the coverslip, capillary adsorbed and the temperature was decreased slowly before examination under the microscope.

Samples for WAXS were prepared inside glass capillaries (Mark-Röhrchen, Germany). Measurements were carried out at the XRD-1 beamline at the Brazilian Synchrotron Light Laboratory (LNLS) in Campinas, Brazil at room temperature (25 °C). Data collection was performed with a system consisting of 24 detectors (MYTHEN 24K from Dectris) that covered 120°, and was carried out in two steps in order to overcome the gaps between the individual detectors.

FTIR was performed in a Nicolet 5700 spectrophotometer (Thermo Nicolet) equipped with a DTGS detector and dry-air purge (Parker-Balston). Lipid samples were prepared in 145 mM NaCl

dissolved in D_2O at a final concentration of 5 mg.mL^{-1}. A transmission liquid cell (Harrick Sci) equipped with CaF_2 windows and 56 μm PTFE spacers, was loaded with 23 μL of the lipid dispersions. Absorbance measurements were obtained by averaging 32 spectra at a resolution of 2 cm^{-1}.

3. Results

3.1. DSC

Ceramide *N*-acylated with decanoic acid (C10:0 ceramide) has not, to our knowledge, previously been studied by DSC, although thermograms of ceramides with shorter and longer N-acyl chains have been reported [12, 14, 18, 22]. Due to difficulties in preparation of C10:0 ceramide dispersions a quantitative loading of the DSC cell was not reliable, thus values of ΔCp are not reported. Thermograms of C10:0 ceramide showed asymmetric and rather noisy peaks with a weak exotherm at 60 °C and a main endotherm at 75 °C (Figure 2).

3.2. SAXS

Dispersions of C10:0 ceramide at temperature below 75 °C presented a SAXS pattern with isotropic peaks at positions centered at 0.99-1.00, 1.73, 2.03 and 2.70 nm^{-1} (Figure 3A). The latter did not indicate a lamellar arrangement as previously reported for other ceramides, because peak positions did not follow a whole number ratio as in typical lamellar phases. In fact, they are in a sequence 1, √3, √4 and √7 (Figure 3A), which is produced by lipids in hexagonal phase, probably inverted HII phase, as discussed below. Miller indexes 100, 110, 200 and 210 of HII and SAXS pattern of C10:0 Ceramide followed a correlation higher than 0.99 as shown in the Figure 3B. No hexagonal phase has been reported before for a ceramide *N*-acylated with a non-hydroxylated

fatty acid [17], even though the critical packing parameter (CPP) of ceramides should allow formation of inverted mesophases [9].

The position of the first order peak at 0.99-1.00 nm^{-1} indicates that the distance *d* between periodic planes of the putative hexagonal phase ($d=2\pi/q$) is 6.3 nm whereas the distance *a* between the center of the hexagonal array of cylinders ($a=2\pi/q$*cos 30°) is 7.3 nm.

The diffraction pattern did not change upon heating from 50 to 72 °C (Figure 3A), indicating a negligible thermal expansivity of the lipid dispersion. The lack of the negative thermal expansion usually observed in membranes [26] suggests a predominance of *trans* conformers in the acyl chains of C10:0 ceramides (see below).

At 82 °C, the ceramide structure melted in a disordered phase, with a single, strong and wide reflection expanding from 1.25 to 3.3 nm^{-1} and centered at higher q values (2.15-2.2 nm^{-1}, Figure 3A), corresponding to a plane periodicity of ~2.9 nm. The latter values and interpretation as a disordered phase concur with previous work on ceramides with long, α-hydroxylated *N*-acyl chains [17]. This behavior was a consistent and very reproducible feature among the independent experiments that were carried out (N=4).

The diffuse and broad signal at 82°C probably represents the form factor of the uncorrelated tubular micelles. Alternatively, since it is very wide, it can be a diffraction peak of the melted state, with a coherence length of 6 nm, which is about two *d* spacings of 2.9 nm. In this case, the position of the peak stands for a very thin, melted structure.

3.3. PLM

In order to further inspect the ceramide arrangements we carried out polarized light microscopy at room temperature of C10:0 ceramide films that were hydrated in glass slides at temperatures above the transition. Pictures in Figure 4 indicate that C10:0 ceramide films under crossed

polarizers illumination display a fan-like texture, typical of hexagonal phases [27, 28], supporting the idea of a hexagonal type of arrangement of the short-chain ceramide in tubular micelles at temperatures below that of the main transition.

3.4. FTIR

Inverted hexagonal phases have been previously observed only in lipids with melted hydrocarbon chains (in a disordered acyl chain configuration). Here we undertook a conformational study of the C10:0 ceramide molecules by means of infrared spectroscopy. FTIR spectra of C10:0 ceramide dispersions in 145 mM NaCl prepared in D_2O showed low wavenumber values for the symmetric stretching vibrations of methylene groups, typical of lipids that are in ordered state (Figure 5). The wavenumber values remained almost unchanged over the temperature range of 20-40 °C but slightly increased at 40-60 °C (Figure 5), suggesting an increasing ratio of *gauge/trans* conformers along the acyl chains. Nevertheless, the frequency range, band shape and width remained closer to those of ordered acyl chains (in comparison to those of disordered acyl chains), denoting a solid/solid transition similar to those observed in other ceramide studies [29]. At temperatures higher than 73 °C, a steep increase of the frequency of the stretching vibrational modes of methylene groups, as well as broadening of the bands (Figure 5), both indicate the melting of the acyl chains, in agreement with the main endothermic peak of the DSC trace (Figure 2).
The Amide I' vibrational mode, on the other hand, showed band splitting at temperatures below that of the main transition, showing a low frequency component located near 1600 cm^{-1} and a higher frequency component at 1628 cm^{-1} (Figure 5). The different components may arise from amide groups hydrogen bonded with different strength. Studies of longer *N*-acyl chain ceramides ascribed the lower frequency componentto intermolecular interactions at the interfacial level

between ceramides molecules in a solid/gel state [30]. By increasing the temperature from 20 to 40 °C, the overall Amide I' band remained split and almost unaltered, but at temperatures above 45 °C and below 73 °C, the low frequency Amide I component band shifts to higher frequency. At 73 °C, the component bands of the Amide I' vibrational mode collapsed into a single broad asymmetric band (Figure 5).

Amide I' band splitting would not be produced by partially hydrated samples, despite the difficulty in obtaining clear lipid dispersion upon ceramide hydration. The protocol described in Section 2 ensure the maximal hydration of the sample, as suggested by the absence of Amide II in the spectra (data not shown), which indicates that all the amide groups have exchanged their protons by deuterons (D/H exchange), *i.e.*, the interfacial region of the lipid assembly is completely hydrated.

3.5. WAXS

The configuration of acyl chains was also evaluated by means of WAXS in an independent setup at room temperature, which is below the main endothermic transition observed in DSC measurements. Diffraction measurements revealed a complex pattern consisting in sharp peaks characteristics of ordered acyl chains (Figure 6). The major peak at 1.50 $Å^{-1}$ indicated a plane periodicity of 4.2 Å. The main peak also showed a shoulder at 1.57 $Å^{-1}$ (4.0 Å in real space) that can be produced by distortions of the hexagonal array, also called (disordered) orthorhombic [31, 32]. Additionally, a minor broad peak at 1.44 $Å^{-1}$ (4.4 Å in real space) was also observed indicating a fraction of less packed acyl chains.

4. DISCUSSION

In order to rationalize the present results of C10:0 ceramide in bulk, we will first take into account the surface behavior of C10:0 ceramide in planar Langmuir monolayers and compare them with C16:0 sphingomyelin. Previous studies in Langmuir monolayers had demonstrated that C10:0 ceramide at 24 °C showed an expanded to condensed transition [21] at about 25 $mN.m^{-1}$, a surface pressure value higher than the transition pressure of C16:0 sphingomyelin [22, 23, 33, 34] which is about 12 $mN.m^{-1}$. This fact implies a less solid character of the short chain ceramide compared to the symmetric sphingomyelin. However, this trend is not followed by the behavior of the same lipids in bulk. The main transition temperature of C10:0 ceramide when dispersed in bulk is higher than that of C16:0 sphingomyelin [34] (75 °C vs 41 °C, respectively) indicating a less solid character of the sphingomyelin in this case. Thus, this proposes that the arrangement of the molecules in the planar geometry imposed in monolayers at the air-water interface is not preserved in C10:0 ceramide when dispersed in bulk, at variance with the bilayer forming C16:0 sphingomyelin (data not shown).

Indeed, by means of both, polarized light microscopy and SAXS, we were able to ascertain that C10:0 ceramide molecules arranged in hexagonal phase at temperatures below the main transition. The first (100) and third (200) SAXS peaks were of low intensity, up to two orders of magnitude weaker than the strongest second (110) peak, thus impairing its observation in measurements with low S/N ratio. In fact, the first minor peaks could only be observed in samples where the major peak reached an intensity of two orders of magnitude above the baseline. The composite SAXS signal is equal to

$$I_q = F_q.S_q$$

where *F(q)* is the form factor, the signal arising from interference of individual tubular micelles; and *S(q)* is the structure factor, the interference function from correlated micelles. Thus, a node in the form factor around 1 nm^{-1} (probably related to the red curve in Fig. 3A) will make any diffraction peak at this position to almost vanish (blue and brown curves in Fig. 3A). We speculate that the low intensity of the first order peak is produced by the form factor, which would reach a node at its *q* position (see Fig 17 in [35]). Certainly, scattering simulations results of a hypothetical micellar model (see below) implied that such a node of the form factor *F* at $1nm^{-1}$ is formed (see Fig 8 below). On the other hand, it should be noticed that other hexagonal systems not following the canonical distribution of intensity of the peaks has been reported [35, 36]. These last systems are similar to our case in the fact that the peak 110 is of the highest intensity whereas the peak 100 is very weak. The contribution of the form factor is usually underestimated, but in systems with low correlation, *F* can contribute even more heavily than *S,* the interference function, thus modulating Bragg peaks.

The X-ray repeat distance *d* could be used for calculation of the lattice spacing *a* of the HII phase (the spacing distance between the centers of the aqueous regions of the inverted cylinders) and this was 7.3 nm. If we assume that ceramide molecules are stretched and partially interdigitated, and we take into account both the planar configuration of the amide bond and the fact that the carbons below the allyl group at position 4,5 of the sphingosine base do not contribute to the hydrophobic region of the molecule [37], then the length of the acyl chains [9] between the water channels should be formed by the terminal methyl groups of the opposed inverted micelles, considering 14 methylene groups of the sphingosine chain and 8 methylene groups of the N-acyl chain:

$$l_{HC} = \left(0.15 \, nm/CH_3 \times 2 \; CH_3 \right) + \left(0.127 \, nm/CH_2 \times (14+8) CH_2 \right) \sim 3.1 \, nm$$

According to X-ray reflectivity measurements in floating monolayers, the length of two ceramide headgroups is 0.9 nm [38]. Then, the length of two apposed ceramides would be 4.0 nm. Thus, the diameter of the aqueous internal channel would be

$$d_w = 7.3 \, nm - 4.0 \, nm \sim 3.3 \, nm$$

Taking into account that the polar head group of ceramides is highly dehydrated, the latter represents a wide channel which could accommodate about 5.5 water layers from the border to the center, much more than the amount of water needed for hydration. We speculate that the role of water could be to alleviate high curvature and packing frustration between cylinders (see below).

Upon heating up to 70 °C, the SAXS pattern did not change. Fluid phases are responsive to heating due to decay in trans/gauche ratio and lateral expansion as temperature increase, determining a negative thermal expansivity normal to the lipid layers [26]. The lack of change in the *d* spacing suggests a solid/gel state of the ceramide at temperatures below 70 °C.

FTIR spectroscopy indicated that at temperatures below 75 °C, the methylene groups of the acyl chains of C10:0 ceramide showed a high proportion of *trans* isomers, typical of gel/solid states. The splitting of the Amide I' band also indicates a high order degree of ceramide molecules at the interfacial region of the aggregates. This is also supported by the absence of the Amide II band in the 1600-1500 cm^{-1} spectral region, denoting full H/D exchange and thus total hydration of the interfacial region, precluding the assignment of the Amide I' band splitting to a partial hydration issue. Previous studies with ATR-FTIR in multilayers of C16:0 ceramide at temperatures below chain melting showed the same kind of band splitting [30], and was explained to be a consequence

of the intermolecular coupling of the Amide I mode when strong hydrogen bonding involves the amide bonds in ceramide films in solid/gel phase. Amide I band splitting has also been observed in extended secondary structural motives in polypeptides and proteins, in which inter-chain hydrogen bonds are formed between the CO and NH of the peptide backbone [39, 40]. In addition, the wavenumber values of the Amide I' peaks of C10:0 ceramide are actually quite low when compared to Amide I peaks of peptides and even with those of longer chain ceramides [30], suggesting a stronger network of hydrogen bonds between amide groups [29] of the asymmetric short chain ceramide. Thus, both the frequency of methylene groups stretching and the splitting and frequency of the Amide I' band indicate that in the hexagonal type II phase in which the C10:0 ceramide is arranged, the molecules are in an all-trans closely packed state.

The sharp peak in the WAXS region at 1.5 $Å^{-1}$ confirmed the high order degree of the acyl chains at temperatures where SAXS and polarizing microscopy indicated the occurrence of inverted hexagonal phase of the C10:0 ceramide molecules. In fact, the peak at 1.57 $Å^{-1}$ typically evinces a distorted hexagonal lattice of the acyl chains [31, 41].

At temperatures higher than the exothermic peak at 60 °C and below 75 °C, hydrocarbon chain begin to increase its proportion of gauge conformers, as revealed by infrared spectroscopy, along with an increase in wavenumber of the low frequency peak of the Amide I' mode, also indicating a weakening of the vibrational coupling and increase of the hydrogen bond network in the interfacial zone of ceramides. However, the wavenumbers of both vibrational modes remain in values typical of ordered phases. Interestingly, methylene bands became more intense than in the spectra measured below 50 °C whereas, according to SAXS, the lipid dispersion remains in HII phase. The exothermic transition with partial melting between HII phases observed in C10:0 ceramide is in opposition to the strong endothermic melting in bilayers, like Lc-Lα, Lβ-Lα or Lβ-HII

phase transitions. However, partially melted hydrocarbon chains would contribute to reduction of the packing frustration in void volumes that are present between the inverted cylinders in hexagonal II arrangements, allowing the acyl chains to adapt more easily to the geometrical impositions of cylinder packing (see below). In fact, WAXS at room temperature also shows (besides the clear predominant peaks for ordered chains) a broad peak centered at 1.435 $Å^{-1}$, produced by a population of liquid like acyl chains or fragments of them. It is worth recalling that Amide bonds remain coupled up to 75 °C, indicating that the interfacial region of the reversed cylinders that form the HII phase remains structured. By increasing the temperature beyond the endothermic peak at 75 °C, melting of the acyl chains and decoupling between the cylinders occurred, as indicated by: 1) the loss of HII pattern in SAXS spectra, 2) the absence of coupling of the Amide I mode and 3) the broadening of the methylene symmetric stretching band.
According to the Critical Packing Parameter (CPP > 1), ceramides would be prone to form inverted phases owing to its small and low hydrated polar headgroup, the presence of H bonding in the interfacial region and the absence of coulombic repulsion due to lack of charged groups (that could reduce interfacial tension) [35], as in the case of phosphatidylethanolamines, in which hexagonal II phases have been extensively studied [42]. However, only ceramides N-acylated with α-hydroxylated fatty acids have been reported to form hexagonal II phases and only when heated above the main chain melting transition temperature [17]. When mixed with DEPE, long but not short N-acyl chain ceramides decreased the Lα-HII transition temperature in a concentration dependent manner [14], showing that long chain ceramides increased the negative curvature of the bilayer formed by the glycerophospholipid and stabilize the HII phase. Also, egg ceramide when mixed with egg-sphingomyelin induced formation of cubic phase at both high temperatures and ceramide contents in binary mixtures [43]. However, in all these cases, the inverted phase was

formed only with hydrocarbon chains in disordered state, either by a coupling of the chain melting process with a bilayer to non-bilayer rearrangement in a Lc-HII transition, as in the case of the N-hydroxy-acyl ceramide; or by a phase transformation from an already melted bilayer as in the case of the most common Lα-HII transitions. Thus, the inverted phase formed by C10:0 ceramide would be the first reported hexagonal type II phase with molecules arranged in ordered state, and probably responds to other mechanism than that of the classical wedge-shaped lipid.

A challenging issue is to explain how this short chain ceramide manages to fill or reduce the acyl chains packing frustration that arises from the "void" volume in between the inverted cylinders that constitute the HII structure. In this regard, the asymmetry between the length of hydrocarbon chains of the sphingosine base and the N-linked fatty acid may play a significant role by reducing the packing frustration typical of inverted hexagonal phases [35, 44, 45] by stretching of the sphingosine chain into this space, thus reducing the "void" volume (Fig. 7). In other words, the terminal methyl of sphingosine may extend over the interstitial matrix between the cylinders, reducing the empty space of the voids (Fig. 7). At the contact zone between cylinders, the asymmetric ceramide molecules could show full or partial interdigitation of extended hydrophobic moieties, or even adopt alternative bent conformations like that proposed in Langmuir monolayers [21] where closer apposition of the hydrophobic regions occur. The diameter of water channel should optimally be adapted to fulfill both the curvature of the interface and the sphingosine chain to reach the center of the frustration volume, relieving stress for the formation of the inverted hexagonal phase: wider water channels would impair sphingosine chains reaching into the void space (Fig. S1), whereas thinner water channels would not be able to accommodate the hydrocarbon chains in the hydrophobic volume between the tubular micelles, as a result of steric/entropic repulsion. It is worth mentioning that the diameter of the water channel of C10:0

ceramide dispersion, although higher than needed for lipid headgroup hydration, is smaller than those of hexagonal phases formed by phosphatidylethanolamines, for example [46].

Taking into account the proposed model and the electron densities calculated from X-ray reflectivities measurements of ceramide films [38], we calculated the form factor of our hypothetical model by means of an inverse Fourier transform approach [25]. We found that only minor modifications of the model of Figure 7 were necessary to capture an essential feature of the C10:0 Ceramide SAXS signal; that is, lipidic reverse micelles with 2.15 nm wall thickness surrounding water channels of 3.3 nm in diameter, diminished the intensity of the first and third diffraction (100) (200) peaks due to nodes (or zeros) in the form factor at those position (Fig 8). Similar results have been reported in calculations where the first order diffraction peak can become very weak, Fig 17 in [35]. Although our simulation data did not allow us to calculate a detailed electron density profile, it captures its essential and unusual feature of having a low intensity first order diffraction peak. Additionally, the simulations confirmed that the micellar topology was typical of an inverse arrangement and not a direct, HI hexagonal phase. The simulated form factor for the direct (HI) micelle has the minimum very far away from the first (100) peak, probing that the electron density distribution of the direct micelle but the inverse one corresponds with our SAXS data.

As a corollary of this work the usual first interpretation of X-ray scattering, which assumes a lamellar array even when relation between peaks does not follow a clear relation of whole numbers as expected for lamellar systems [26], should be revised. In the case of C10:0 ceramide, the SAXS pattern clearly does not correlate with a lamellar arrangement. In a hexagonal array the distance between successive crystallographic planes is $2\pi/q_1$, as in the lamellar phase, but the

distance between the center of adjacent micelles is $2d^*(3^{1/2})$ [47, 48], which is about 13% larger if we assume a lamellar array. Then, if the assigned lattice were wrong, a considerable source of error would arise when building supramolecular models of aggregated ceramide extending beyond the lattice itself. A further complication appears when the first and third peaks are faint and difficult to measure so only synchrotron source for SAXS must be used. The second major point is that this hexagonal phase persists even at low temperatures at which acyl chains are frozen and also in a hexagonal array, according to WAXS data. To our knowledge this is the first time that a hexagonal phase with ordered acyl chains is reported in lipid systems.

As a final remark, asymmetry in lipid molecular shape as a consequence of mismatch between the length of the acyl chains has been generally recognized as a determinant of new lipid arrangement, like the interdigitation of PC membranes [49].However, it was not extensively studied in molecular species of sphingolipids, where acyl chain length asymmetry is commonly found in lipids isolated from natural sources. Ongoing work indicates that asymmetry facilitates interface curvature in ceramides, which would affect biomembranes curvature, where ceramide can be enzymatically formed from the bilayer forming sphingomyelin [50]. The activity of sphingomyelinases can be in turn modulated by the changes in curvature induced by its own product, ceramide.

5. **Conclusions**

The asymmetric short chain sphingolipid C10:0 ceramide formed an inverted hexagonal HII phase at full hydration conditions and at temperatures below the main endothermic melting transition. This novel phase with ordered chains is formed as lipid asymmetry reduces the void volumes between the lipid tubules arranged in hexagonal lattice.

Acknowledgements

RGO thanks to the Brazilian Synchrotron Light Laboratory (CNPEM/MCT) for X-ray beamtime at SAXS-2 beamline (projects D11A – SAXS1 – 10716 and 16019), and at the XRD-1 beamline.

Dr Víctor M Galván Sosa (FaMAF-UNC/CONICET) is acknowledged by his assistance in modelling of the SAXS data and for helpful discussions. The technical assistance of Mr Rafael Gutierrez (Centro Científico Tecnológico-CONICET/Tucumán) for the setting up of infrared spectrometer and experiments is acknowledged.

This work was supported with grants from FONCyT, CONICET, and SECyT-UNC. RGO, BM and FGD are members are researchers from CONICET. SPFB is a CONICET fellow.

References

[1] F.M. Goñi, A. Alonso, Biochim Biophys Acta, 1758 (2006) 1902-1921.
[2] Y.A. Hannun, R.M. Bell, Science, 243 (1989) 500-507.
[3] R. Koynova, M. Caffrey, Biochim Biophys Acta, 1255 (1995) 213-236.
[4] B. Maggio, Prog Biophys Mol Biol, 62 (1994) 55-117.
[5] B. Maggio, G.A. Borioli, M. Del Boca, L. De Tullio, M.L. Fanani, R.G. Oliveira, C.M. Rosetti, N. Wilke, Cell Biochem Biophys, 50 (2008) 79-109.
[6] B. Maggio, D.C. Carrer, M.L. Fanani, R.G. Oliveira, C.M. Rosetti, Current Opinion in Colloid & Interface Science, 8 (2004) 448-458.
[7] D.A. Peñalva, G.M. Oresti, F. Dupuy, S.S. Antollini, B. Maggio, M.I. Aveldaño, M.L. Fanani, Biochimica et Biophysica Acta (BBA) - Biomembranes, 1838 (2014) 731-738.
[8] B. Maggio, M.L. Fanani, C.M. Rosetti, N. Wilke, Biochim Biophys Acta, 1758 (2006) 1922-1944.
[9] J.N. Israelachvili, Chapter 20 - Soft and Biological Structures, Intermolecular and Surface Forces (Third Edition), Academic Press, San Diego, 2011, pp. 535-576.
[10] L. Cantu, E. Del Favero, P. Brocca, M. Corti, Adv Colloid Interface Sci, 205 (2014) 177-186.
[11] B. Maggio, Biochim Biophys Acta, 815 (1985) 245-258.
[12] J. Shah, J.M. Atienza, R.I. Duclos, Jr., A.V. Rawlings, Z. Dong, G.G. Shipley, J Lipid Res, 36 (1995) 1936-1944.
[13] B. Maggio, J. Albert, R.K. Yu, Biochim Biophys Acta, 945 (1988) 145-160.
[14] J. Sot, F.J. Aranda, M.I. Collado, F.M. Goñi, A. Alonso, Biophys J, 88 (2005) 3368-3380.
[15] D.C. Carrer, B. Maggio, J Lipid Res, 40 (1999) 1978-1989.
[16] G.D. Fidelio, B. Maggio, F.A. Cumar, Biochim Biophys Acta, 854 (1986) 231-239.
[17] J. Shah, J.M. Atienza, A.V. Rawlings, G.G. Shipley, J Lipid Res, 36 (1995) 1945-1955.
[18] B. Westerlund, P.M. Grandell, Y.J. Isaksson, J.P. Slotte, Eur Biophys J, 39 (2009) 1117-1128.
[19] I. López-Montero, F. Monroy, M. Velez, P.F. Devaux, Biochim Biophys Acta, 1798 (2010) 1348-1356.
[20] B.M. Castro, M. Prieto, L.C. Silva, Prog Lipid Res, 54 (2014) 53-67.
[21] F. Dupuy, M.L. Fanani, B. Maggio, Langmuir, 27 (2011) 3783-3791.
[22] J.V. Busto, M.L. Fanani, L. De Tullio, J. Sot, B. Maggio, F.M. Goñi, A. Alonso, Biophys J, 97 (2009) 2717-2726.
[23] F.G. Dupuy, B. Maggio, J Phys Chem B, 118 (2014) 7475–7487.
[24] S.N. Pinto, L.C. Silva, A.H. Futerman, M. Prieto, Biochim Biophys Acta, 1808 (2011) 2753-2760.
[25] K. Schmidt-Rohr, Journal of Applied Crystallography, 40 (2007) 16-25.
[26] J.M. Seddon, R.H. Templer, Chapter 3 - Polymorphism of Lipid-Water Systems, in R.Lipowsky and E. Sackmann (Eds), Handbook of Biological Physics, North-Holland, 1995, pp. 97-160.
[27] J. Borné, T. Nylander, A. Khan, Langmuir, 16 (2000) 10044-10054.
[28] N.J. Brooks, H.A.A. Hamid, R. Hashim, T. Heidelberg, J.M. Seddon, C.E. Conn, S.M. Mirzadeh Husseini, N.I. Zahid, R.S.D. Hussen, Liquid Crystals, 38 (2011) 1725-1734.
[29] P. Garidel, Physical Chemistry Chemical Physics, 4 (2002) 1934-1942.
[30] D.J. Moore, M.E. Rerek, R. Mendelsohn, The Journal of Physical Chemistry B, 101 (1997) 8933-8940.
[31] M.J. Janiak, D.M. Small, G.G. Shipley, Biochemistry, 15 (1976) 4575-4580.
[32] M.J. Janiak, D.M. Small, G.G. Shipley, J Biol Chem, 254 (1979) 6068-6078.
[33] J.M. Smaby, V.S. Kulkarni, M. Momsen, R.E. Brown, Biophys J, 70 (1996) 868-877.
[34] B. Ramstedt, J.P. Slotte, Biophys J, 77 (1999) 1498-1506.

[35] J.M. Seddon, Biochim Biophys Acta, 1031 (1990) 1-69.
[36] A. Picco, M. Kraska, H. Didzoleit, C. Appel, G. Silbestri, O. Azzaroni, B. Stuhn, M. Ceolín, J Colloid Interface Sci, 436 (2014) 243-250.
[37] I. Pascher, Biochim Biophys Acta, 455 (1976) 433-451.
[38] D. Vaknin, M.S. Kelley, Biophys J, 79 (2000) 2616-2623.
[39] E. Goormaghtigh, V. Cabiaux, J.-M. Ruysschaert, Determination of Soluble and Membrane Protein Structure by Fourier Transform Infrared Spectroscopy, in: H.J. Hilderson, G.B. Ralston (Eds.) Physicochemical Methods in the Study of Biomembranes, Springer Science, Business Media, New York, 1994, pp. 329-362.
[40] N. Kucerka, J.F. Nagle, J.N. Sachs, S.E. Feller, J. Pencer, A. Jackson, J. Katsaras, Biophys J, 95 (2008) 2356-2367.
[41] P. Laggner, X-Ray Diffraction on Biomembranes with Emphasis on Lipid Moiety, in: H.J. Hilderson, G.B. Ralston (Eds.) Physicochemical Methods in the Study of Biomembranes, Springer Science, Business Media, New York, 1994, pp. 451-491.
[42] J.M. Seddon, G. Cevc, R.D. Kaye, D. Marsh, Biochemistry, 23 (1984) 2634-2644.
[43] H.M. Barriga, E.S. Parsons, N.L. McCarthy, O. Ces, J.M. Seddon, R.V. Law, N.J. Brooks, Langmuir, 31 (2015) 3678-3686.
[44] G.L. Kirk, S.M. Gruner, D.L. Stein, Biochemistry, 23 (1984) 1093-1102.
[45] P.M. Duesing, R.H. Templer, J.M. Seddon, Langmuir, 13 (1997) 351-359.
[46] D. Marsh, X-Ray Diffraction Data and Cylinder Diameters for HII (and HI) Phases, Handbook of Lipid Bilayers, CRC Press, Boca Raton, London, New York, 2013.
[47] V. Luzzati, X-Ray Diffraction Studies of Lipid-Water Systems, in: D. Chapman (Ed.) Biological Membranes: Physical Fact and Function, Academic Press, London and New York, 1968, pp. 71-123.
[48] D.C. Turner, S.M. Gruner, Biochemistry, 31 (1992) 1340-1355.
[49] C. Huang, J.T. Mason, Biochim Biophys Acta, 864 (1986) 423-470.
[50] M.B. Ruiz-Argüello, G. Basáñez, F.M. Goñi, A. Alonso, J Biol Chem, 271 (1996) 26616-26621.

Figure captions

Figure 1. Chemical structure of *N*-decanoyl- D-*erythro*-sphingosine (C10:0 ceramide)

Figure 2. DSC thermal trace of C10:0 ceramide at a nominal concentration of 0.5 $mg.mL^{-1}$. A clear endothermic peak is observed at 75°C, a less pronounced exothermic peak is observed at 60 °C. Scans were performed at 0.5 $°C.min^{-1}$ in triplicate independent samples. A representative scan is shown.

Figure 3.**A.** SAXS patterns of C10:0 ceramide at the indicated temperatures in the hexagonal phase (blue and brown) and disordered phase (red). Synchrotron radiation was used and spectra were acquired after 10 min of thermal stabilization. Measurements were carried out in triplicate with fresh samples. **B.** Correlation of the position of the SAXS peaks with Miller indexes of a hexagonal crystal array.

Figure 4. Hydrated lipid films of C10:0 ceramide were imaged by polarized optical microscopy at a magnification of 400X. A) and B) are duplicates.

Figure 5. FTIR thermal scan of C10:0 ceramide. The center of mass of symmetric stretching of methylene groups band (upper right panel) and of the component peaks of Amide I band (lower right panel) were calculated at different temperatures. Measurements were carried out in triplicate with fresh samples. A representative set of spectra and band position is shown.

Figure 6. WAXS of C10:0 ceramide measured at room temperature. The major peaks at 1.50 and 1.57 Å are indicative of a predominant ordered state of the acyl chains. The minor peak at 1.44 Å accounts for less densely packed chains in fluid-like state. Measurements were carried in duplicate, and a representative spectrum is shown.

Figure 7. Simplified model of the HII tubular micelles represented in cross section. The main slabs are shown in color; blue for water, red ring for polar headgroup, brown ring for the non-interdigitated acyl chain region, yellow ring for the asymmetric (interdigitated) region of the acyl chains, green stick (C10 acyl chain), red stick for the acyl part of sphingosine and white is the packing frustration region. The remarkable feature of this cartoon is that the sphingosine methyl end practically fit close to the center of the space between the cylinders, relieving packing frustration.

Figure 8. Scattering factors obtained starting from HII micelle model of Fig 7. A deep minimum at 1 nm^{-1} is obtained for the Form factor (black curve). This minimum damps the predominant structure factor peak (blue curve) in the resulting SAXS signal (red curve) at the same position.

Figure 1

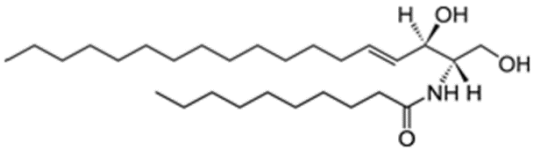

Figure 2

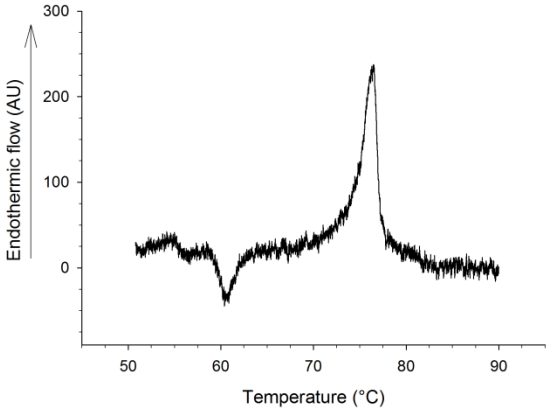

Figure 3

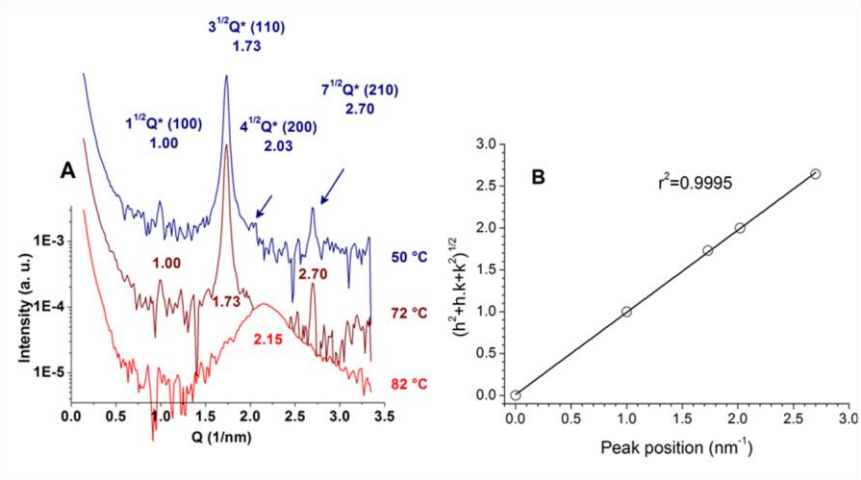

Figure 4

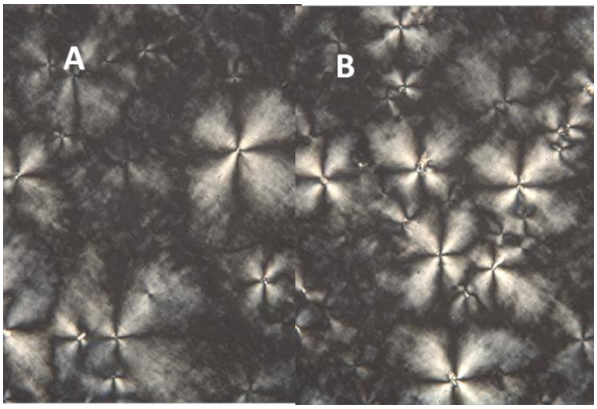

Figure 5.

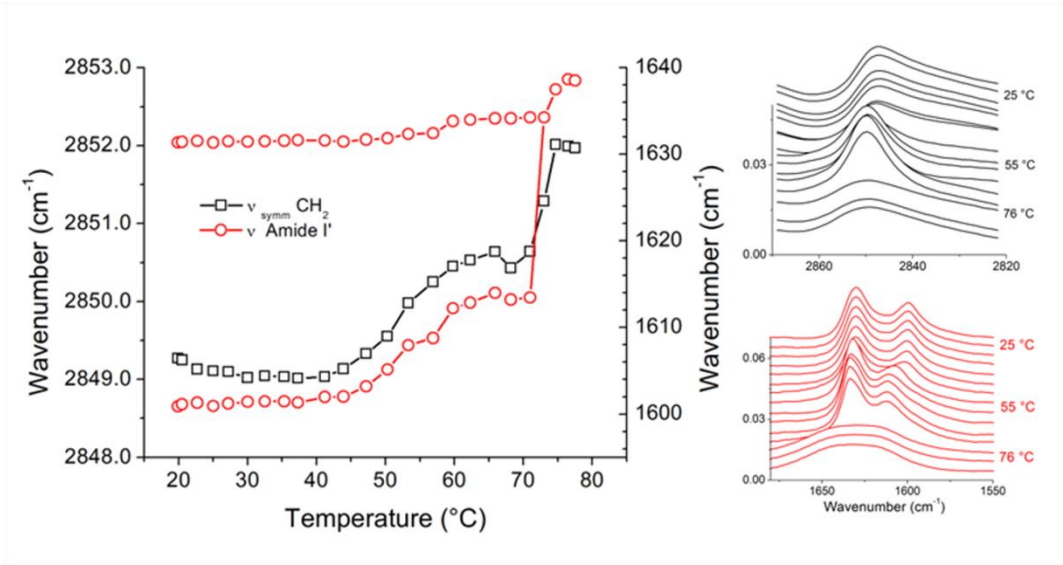

Figure 6.

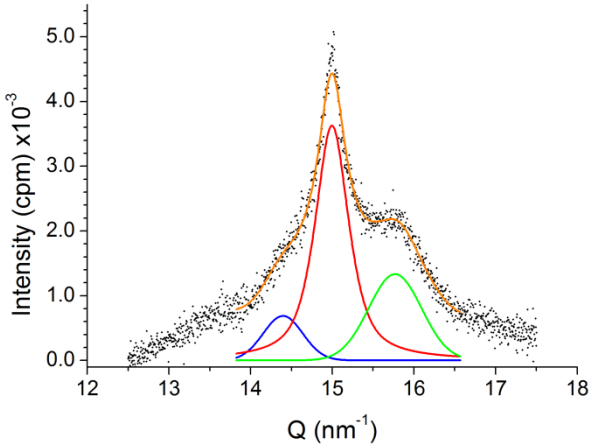

Figure 7

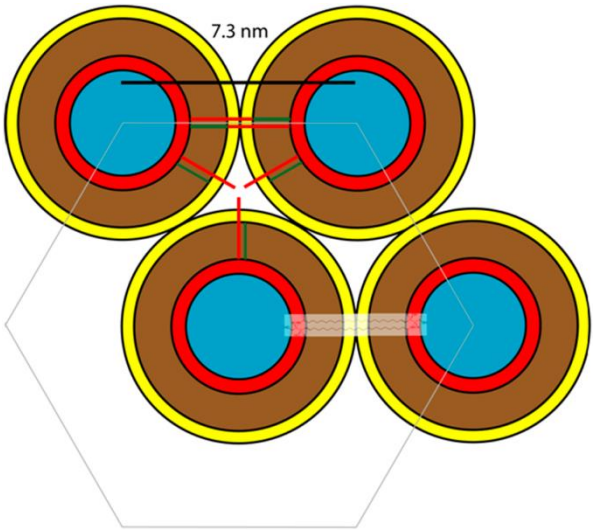

Figure 8.

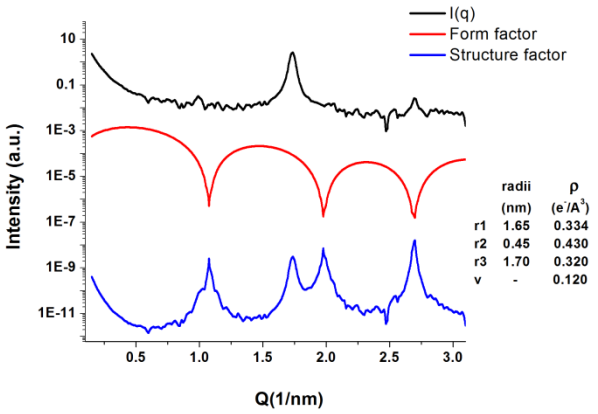
I(q)
Form factor
Structure factor
Intensity (a.u.)
10
0.1
1E-3
1E-5
1E-7
1E-9
1E-11
0.5
1.0
1.5
2.0
2.5
3.0
Q(1/nm)
radii (nm)
ρ (e⁻/Å³)
r1 1.65 0.334
r2 0.45 0.430
r3 1.70 0.320
v - 0.120